A 3.52 Gb/s mmWave Baseband with Delayed Decision Feedback Sequence Estimation in 40 nm

Nicholas Preyss, Christian Senning, and Andreas Burg
School of Engineering
Telecommunications Circuits Laboratory
EPF Lausanne, 1015 Lausanne, Switzerland

Wei-Chang Liu, Chun-Yi Liu, and Shyh-Jye Jou
Department of Electronics Engineering
Institute of Electronics
National Chiao Tung University, Hsinchu, Taiwan R.O.C.

Abstract—We present a digital baseband ASIC for 60 GHz single-carrier (SC) transmission that is optimized for communication scenarios in which most of the energy is concentrated in the first few channel taps. Such scenarios occur for example in office environments with strong reflections. Our circuit targets close-to-optimum maximum-likelihood performance under such conditions. To this end, we show for the first time how a reduced-state-sequence-estimation algorithm can be realized for the 1760 MHz bandwidth of the IEEE 802.11ad standard. The equalizer is complemented in the frontend by a synchronization unit for frequency offset compensation as well as a Golay-sequence based channel estimator and in the backend by an low density parity check (LDPC) decoder. In 40nm CMOS we achieve a measured data rate of up to 3.52 Gb/s using QPSK modulation.

I. INTRODUCTION

With the continuous growth of the Wi-Fi market over the last years, it became apparent that band congestion and the limited throughput are the major obstacles for a further proliferation. Operating at mmWave frequencies seems to be a promising candidate for high-throughput, short-distance wireless applications since large amounts of available spectrum at 60 GHz together with high spectral diversity offer a significant increase in capacity.

The exploration of mmWave for wireless applications goes along with a renaissance of single-carrier (SC) modulation, due to its low requirements on the analog front-end. Many different architectures have been proposed for SC mmWave systems [1]–[4], but to the best of our knowledge, the feasibility of sequence estimation has not been explored for such an application. A full sequence-estimation (SE) results in maximum likelihood (ML) performance and hence exhibits an inherent performance advantage over any linear equalizer in the presence of inter-symbol-interference. Unfortunately, the complexity of full SE easily exceeds feasibility due to its exponential dependency on the delay spread and modulation order. The proposed reduced state SE has the interesting property that it can approach ML performance, while keeping the complexity at a tolerable level.

The paper is structured as follows. In Section II we define the system assumptions for our mmWave receiver. Subsequently in Section III a description of the proposed baseband architecture and the used algorithms is given. Details of the VLSI implementation and measurement results of the fabricated chips are shown in Section IV.

II. SYSTEM CONSIDERATIONS

We assume symbol-spaced samples with a frame-format as specified in the IEEE 802.11ad standard [5] as input. A frame starts with a preamble for synchronization and channel estimation. A 2176 symbol long short training field (STF) offers 17 periodic Golay sequences of length 128 for time and frequency synchronization. The STF is followed by a 1152 symbol long channel estimation field (CEF)
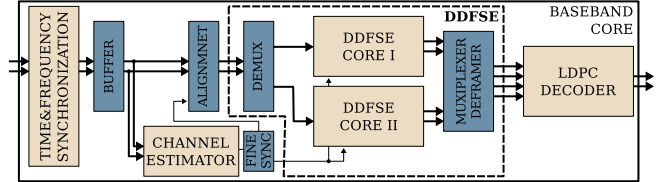
Fig. 1: Block diagram of the proposed 60 GHz baseband based on reduced state sequence estimation.

TABLE I: mmWave Single-Carrier Baseband Overview

DDFSE		
	Modulation	BPSK/QPSK
	Trellis Length	3
	Individual State Feedback	4
	Common History Feedback	22
	11ad pilot support	yes
LDPC		
	Schedule	Layered
	Codeword Size	672
	Code Rate	$\frac{1}{2}/\frac{5}{8}/\frac{3}{4}/\frac{13}{16}$

consisting of two 512 symbol long complementary Golay sequences and a cyclic postfix.

The subsequent payload is structured such that always 448 data symbols are preceded by a fixed pilot word. These pilot words give the payload field a regular block structure which decouples the detection of symbols which are part of different blocks.

III. MMWAVE DDFSE SINGLE-CARRIER BASEBAND

The top-level block diagram of our digital baseband is shown in Fig. 1 with the features summarized in Table I. The design features a synchronization unit for time synchronization and frequency offset (FO) compensation based on the STF of the preamble. A subsequent channel estimation (CE) unit performs time-domain estimation of the channel impulse response (CIR). Equalization and detection of the BPSK or QPSK data symbols of the payload is performed using delayed decision feedback sequence estimation (DDFSE). To this end subsequent blocks of the payload field are buffered and demultiplexed to two soft-output half-rate Radix-2 DDFSE cores. The resulting bitstreams are multiplexed after stripping off the pilot words. The computed log-likelihood ratios for the individual coded payload bits are forwared in chunks of code words to the subsequent LDPC channel decoder.

As the targeted symbol rates for the proposed mmWave system exceeds the clock frequencies for which digital signal processing can be implemented in a power efficient way, the design is based on a 2-way parallel architecture clocked at half the symbol rate.
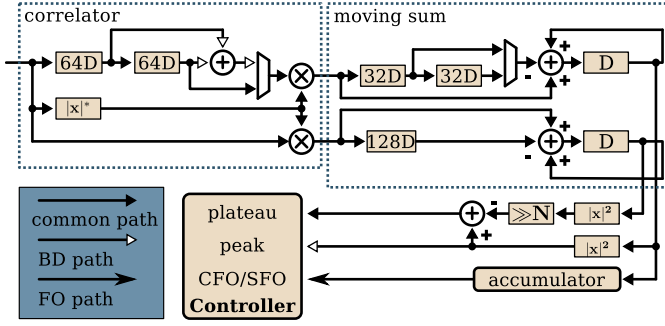
Fig. 2: Block diagram of the auto-correlation based parameter estimation stage in the synchronization unit.

Fig. 3: Bit-error rate (BER) comparison between a 1-tap phase rotater (PR) with DF, a 8-tap linear equalizer (LE) with DF, and the proposed DDFSE in an office environment.

Fig. 4: Block diagram of a basic DDFSE unit without applied architectural transformations (elements identical to a mSOVA are blue).

A. Synchronization & Channel Estimation

A joint preamble/boundary detection (PD/BD) and carrier/sampling frequency offset (CFO/SFO) estimation scheme is proposed in our previous design [6]. The detection and estimation scheme is based on the auto-correlation structure as illustrated in Fig. 2. The structure first uses the normalized auto-correlation with a predefined threshold to detect the start of the preamble. Then it will calculate the phase of auto-correlation part to estimate the FO of the carrier and the sampling. Instead of using the longer length correlation result, this structure adopts the same length-128 (as the size of Golay sequence) delay-line with preamble detection in order to prevent extra delay-line cost. To improve the accuracy of the frequency offset estimation, an accumulator is used to collect the correlation results to reduce the effect of noise. After the detection and estimation procedure, the estimated result is processed to generate 2 ways compensation signals at the same time. Then the interpolator and phase de-rotator compensate the effect of SFO and CFO. The Golay-sequences based CEF of the preamble is forwarded to the channel estimator (CE) in order to perform a time-domain channel estimation. Using Golay sequences for channel estimation as proposed in [7] allows the use of a high-speed, multiplier-free correlation architecture called efficient golay correlator (EGC) [8].

After estimation of the channel impulse response (CIR) the fine synchronization unit aligns the symbol stream to the trellis of the sequence estimation in order to maximize the performance of the sequence estimator. As a power saving measure the fine synchronization unit can additionally mask weak feedback taps of the CIR which are dominated by noise, before passing it to the detector units.

B. Delayed Decision Feedback Sequence Estimation

The implemented DDFSE [9] algorithm approximates the maximum-likelihood solution by limiting the sequence estimation to a reduced state space that covers only the first $D = 3$ taps of the channel. The interference from up to $V = 26$ following, late-arrival (i.e., often weaker) taps is eliminated by an additional decision feedback (DF) stage. The expected interference term from each of the remaining taps is calculated by multiplying the estimated transmitted symbol derived from the decision history with the corresponding channel coefficient and used as feedback term for the input signal.

A bit-error rate (BER) performance comparison of different proposed receivers for mmWave applications in Fig. 3 shows the advantage of the DDFSE over linear equalizers. The simulations are performed with the near-location cubicle (CB) scenario of the IEEE 802.11ad channel model [10], as this would be a typical use case for a mmWave equipped mobile device at the workplace. In this
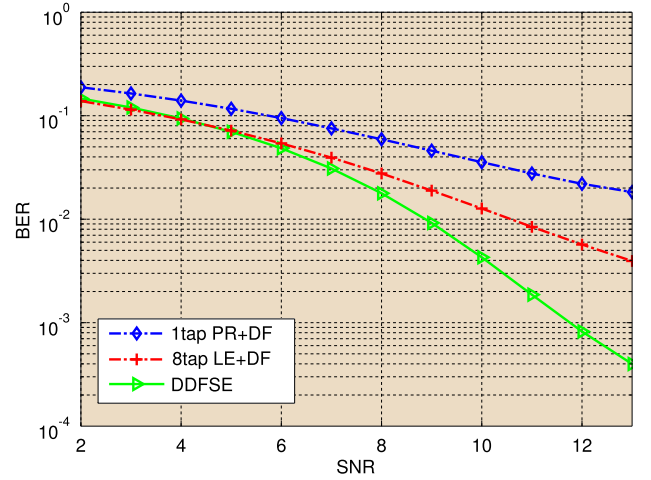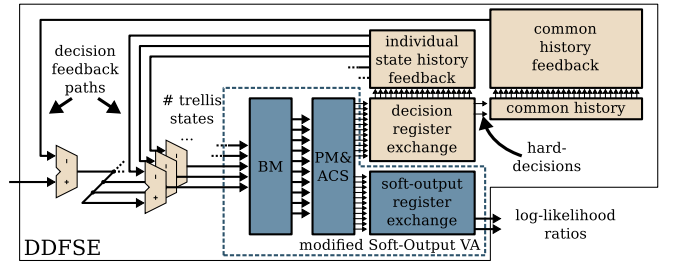
scenario the LOS path is immediately succeeded by strong reflections arising from the compact geometries. The simulations show that the DDFSE can not only exploit the energy of the LOS path but also the energy of subsequent reflections and hence provides significantly better BER performance compared to a 1-tap phase rotator with DF as well as an 8-tap MMSE linear equalizer with DF.

1) Basic Architecture: The straightforward architecture of a DDFSE unit before the necessary architectural transformations to meet timing is depicted in Fig. 4. The hardware consists of a modified soft-output Viterbi Algorithm (mSOVA) unit as proposed in [11] and the components of the additional DF unit.

mSOVA: The mSOVA part comprises a branch metric (BM) unit, a combined add-compare-select and path-metric (ACS/PM) unit with modulo normalization, and a soft-output register exchange. The latter stores the ACS decisions and the differences of the path metrics to compute approximate max-log log-likelihood-ratios [11] for the LDPC decoder during the traceback operation. BPSK modulation is supported by disabling subcircuits that would be required to support QPSK modulation.

Decision-Feedback: The DF stage supports up to $V = 26$ DF taps and is split into an individual state history feedback (ISHF) and a common history feedback (CHF) part to reduce its complexity (with no visible performance penalty). The former comprises only the first $I = 4$ DF taps which are computed individually for each state, while the latter comprises the remaining $V - I = 22$ DF taps where the individual paths have already merged with high probability. The ISHF
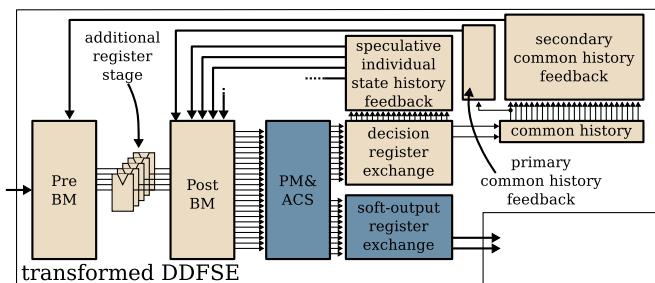
Fig. 5: Block diagram of the optimized DDFSE architecture after rearranging BM operations according to their data dependencies.

comprises a dedicated *decision register exchange* operating in parallel to the soft-output register exchange and an associated *individual state-history feedback* unit. The latter calculates and accumulates a feedback term based on the decision-history for each state to obtain the per-state part of the decision feedback. The common history keeps only a single set of decisions in a shift register that is fed from the first-state output of the *decision register exchange*. The *common history feedback* unit performs the multiply-accumulate operation of these decisions with the associated channel taps to obtain the common history decision feedback value. The segmentation of the decision history in ISHF and CHF lowers the memory requirements by 79%.

2) Optimization for Timing Closure: The architecture in Fig. 4 requires the least number of operations, but timing closure at the half-rate target frequency of 880 MHz is difficult. The critical path is the feedback loop that starts with the computation of the DF terms, continues to the application of the DF to the received samples and through the BM unit and ends in the update of the path metric registers in the ACS/PM unit.

Re-ordering of operations to accommodate late arriving signals, careful re-timing and speculative pre-computation of multiple candidate intermediate results followed by rapid late selection of the correct result are key techniques to remove this timing bottleneck.

As a first measure, we move the computations of the BM of the mSOVA to the beginning of the chain (pre-BM) and add a pipeline register afterwards since this part involves no feedback loops. To also include the subtraction of the late arriving common history decision feedback value in this first pipeline stage, we split the computation of this term into a primary and a secondary component that contains only the first component and all remaining components of the sum-of-products, respectively. The first component can not be retimed and is therefore subtracted after the first pipeline stage, while the late-arriving second component can easily be retimed and can be included in the pre-BM unit. At the cost of 400 instead of 145 arithmetic operations, the proposed latency aware re-ordering of the architecture as shown in Fig. 5 cuts the critical path significantly.

After this retiming, the ISHF path becomes critical, but can not be retimed immediately since each sum-of-products depends directly on the decision outputs of the ACS/PM unit (1st order feedback loop) through the MUXes in the register-exchange (cf. Fig. 6a). Speculative pre-calculation for the four possible feedback values (corresponding to the four possible ACS decisions in case of QPSK) removes this restriction and allows to dedicate an entire cycle to the DF calculation and only a single multiplexer which chooses from precalculated values (cf. Fig. 6b) remains in the feedback path. Interestingly this transformation comes with very little additional complexity, in fact only 16 additional four-way multiplexer and the memory for the feedback signals are added as the number of required sum-product calculations does not change.

Finally, generation of the different feedback signals still requires
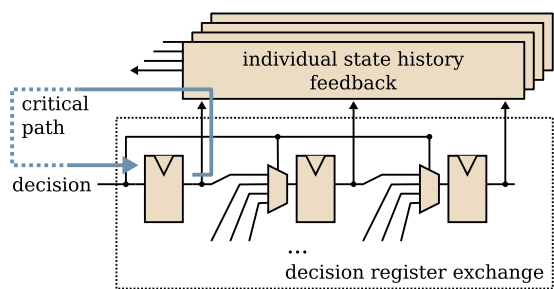
(a) Direct implementation
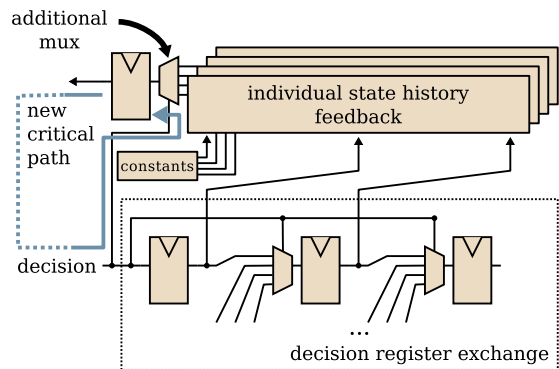
(b) Speculative implementation

Fig. 6: Transformation of the critical path through the ISHF unit by using speculative pre-calculation of possible feedback values.

sums over a considerable number of individual feedback terms, each calculated as product of a channel coefficient with the corresponding decision in the path history. Instead of re-computing these sums-of-products with each update of the corresponding decision histories, the different feedback signals are generated with the help of reconfigurable look-up tables (LUTs). After channel estimation these register-based LUTs are populated with the possible values and subsequently clock-gated during the actual detection phase. Due to the small number of taps, the ISHF is generated by a single LUT, while for the significantly longer CHF, a hybrid approach with the LUTs storing partial sums is used. The LUTs are always initialized for QPSK, for BPSK only a subset is used.

C. Low-density Parity Check (LDPC) Channel Decoder

Channel decoding is performed by a IEEE 802.11ad-compliant soft-input LDPC decoder. The decoder supports a code-word size of 672 bits and all 4 code rates ($\frac{1}{2}/\frac{5}{8}/\frac{3}{4}/\frac{13}{16}$) specified in the standard.

Fast decoding convergence is achieved by using a layered schedule for processing the parity checks. The layered architecture makes use of the quasi-cyclic structure of the LDPC code to process all 42 parity checks of a layer in parallel. In order to achieve the required throughput an additional level of parallelism is required. The columns of the parity check matrices are analyzed and partitioned into two sets. As a result each layer can be processed in two units in parallel and the throughput is nearly doubled.

Double-buffering of the memory structures assures continuous operation. An integrated early termination mechanism saves energy in the high SNR regimes. A more detailed description of the LDPC architecture is given in [12].

IV. VLSI IMPLEMENTATION & MEASUREMENT

The proposed baseband design is fabricated in 40nm CMOS technology. A micrograph of the fabricated chip is shown in Fig. 7.
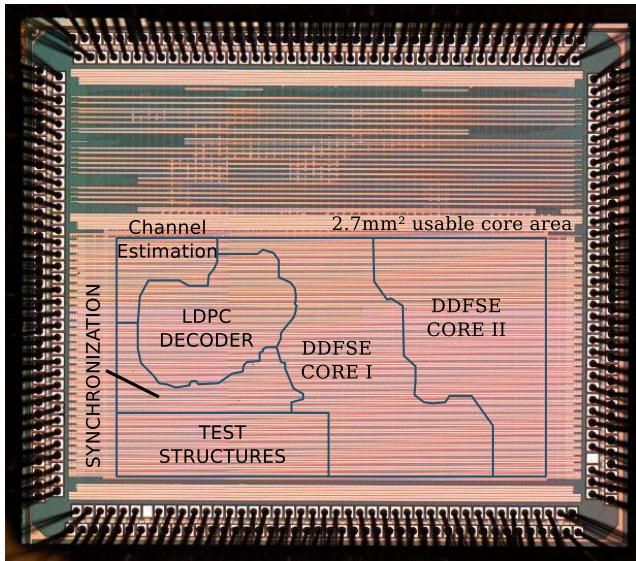
Fig. 7: Micrograph of the manufactured die. The chip accomodates two independent designs in a single pad frame.

TABLE II: Key facts of the VLSI implementation

CMOS Technology	40 nm
Core Area	2.7 mm^2 (Utilization: 67%)
	Synchronization	139 kGE
	Channel Estimator	64 kGE
	DDFSE core I+II	1443 kGE
Gate Count	LDPC Decoder	363 kGE
	Clock Tree	75 kGE
	Reset Tree	25 kGE
	Control&Buffer	97 kGE
	Test Structures	457 kGE
	Total	**2563 kGE**

The available core area is $2.7\,\mathrm{mm}^2$ and the design was placed with a core utilization of $67\,\%$. The core area additionally contains an internal core clock generation and dedicated test structures. Details on the complexity of the different blocks are given in Table II.

The test structure comprises a command buffer and memory for the test vectors to overcome limitations of the I/O interface. The memory is not only used for the input samples of the baseband, but also stores the output of the channel decoder.

Measurements of the fabricated chip were performed in order to verify its correct operation. The required throughput could be achieved with a core supply voltage of $1.15\,\mathrm{V}$. The number constitutes an upper bound, as due to limitations of the measurement setup not all IR-drop on the test setup could be accounted for. The given throughput values specify the raw throughput. Net data rate depend on used pilot word scheme and code rate. The comparison of the results in Table III shows that the proposed DDFSE does not support as high modulation orders as proposed linear equalizer-based basebands, nevertheless for low modulation orders DDFSE can achieve better performance with little additional complexity overhead.

V. CONCLUSION

A full baseband system for single-carrier with synchronization, channel estimation, reduced state sequence estimation based detection and channel decoding could be presented. The system demonstrates the feasibility of sequence estimation for Gb/s wireless systems. Further it was shown that the DDFSE algorithm can provide considerable BER performance gains in small structured environments with strong close-in reflections immediately after the LOS path.

TABLE III: Comparison of mmWave SC receivers

	[1]	[2]	[3]	[4]	This Work
	BPSK	BPSK	BPSK	BPSK	BPSK
	QPSK	QPSK	QPSK	QPSK	QPSK
	16QAM			16QAM	
Sync	no	yes	yes	yes	yes
CE	yes	no	yes	yes	yes
EQ	LE	1-tap	OS-FDE	RLS	DDFSE
DF	yes	no	no	no	yes
Code	no	LDPC	LDPC	LDPC	LDPC
CMOS	65 nm	40nm	40 nm	65 nm	40 nm
core	2.34 mm^2	1.15 mm^2	46.62 mm^{2a}	16 mm^{2b}	2.7 mm^2
rate	2 Gb/s	6.3 Gb/s	1.8 Gb/s	4.6 Gb/s	3.52 Gb/s^c

[a]including ADC/DAC,TX,MAC
[b]including ADC/DAC,TX,uP
[c]at 1.15 V core supply

In order to meet the stringent timing requirements of the system, an architecture based on two half-rate Radix-2 DDFSE cores was implemented. Further speculative pre-calculation combined with re-ordering of arithmetic operations and the introduction of pipeline stages improve the timing of the critical path significantly. Look-up tables with pre-calculated intermediate results are used in the decision feedback section to increase the power efficiency and further reduce the critical path.

A multi-parallel QC-LDPC decoder provides the required channel decoding throughput. Early-termination, clock-gating and a layered processing schedule improves the energy efficiency of the decoder.

REFERENCES

[1] J.-H. Park, B. Richards, and B. Nikolic, "A 2 Gb/s 5.6 mw digital LOS/NLOS equalizer for the 60 GHz band," *IEEE J. Solid-State Circuits*, vol. 46, no. 11, pp. 2524–2534, 2011.

[2] K. Okada *et al.*, "Full four-channel 6.3-gb/s 60-GHz CMOS transceiver with low-power analog and digital baseband circuitry," *IEEE J. Solid-State Circuits*, vol. 48, no. 1, pp. 46 –65, jan. 2013.

[3] N. Saito *et al.*, "A fully integrated 60-GHz CMOS transceiver chipset based on WiGig/IEEE 802.11 ad with built-in self calibration for mobile usage," *IEEE J. Solid-State Circuits*, vol. 48, no. 12, pp. 3146–3159, 2013.

[4] K. Ma *et al.*, "An integrated 60GHz low power two-chip wireless system based on IEEE802.11ad standard," in *Microwave Symposium (IMS), 2014 IEEE MTT-S International*, June 2014, pp. 1–4.

[5] "IEEE standard - part 11 amendment 3: Enhancements for very high throughput in the 60 GHz band," *IEEE Std 802.11ad-2012*, pp. 1–628, Dec 2012.

[6] W.-C. Liu, T.-C. Wei, Y.-S. Huang, C.-D. Chan, and S.-J. Jou, "All-digital synchronization for SC/OFDM mode of IEEE 802.15.3c and IEEE 802.11ad," *IEEE Trans. Circuits Syst. I*, vol. 62, no. 2, pp. 545–553, Feb 2015.

[7] R. Kimura *et al.*, "Golay sequence aided channel estimation for millimeter-wave WPAN systems," in *Personal, Indoor and Mobile Radio Communications, 2008. PIMRC 2008. IEEE 19th International Symposium on*. IEEE, 2008, pp. 1–5.

[8] B. M. Popovic, "Efficient golay correlator," *Electronics Letters*, vol. 35, no. 17, pp. 1427–1428, 1999.

[9] A. Duel-Hallen and C. Heegard, "Delayed decision-feedback sequence estimation," *IEEE Trans. Commun.*, vol. 37, no. 5, pp. 428–436, 1989.

[10] A. Maltsev *et al.*, *Channel Models for 60 GHz WLAN Systems*, 8th ed., IEEE, May 2010. [Online]. Available: https://mentor.ieee.org/802.11/dcn/09/11-09-0334-08-00ad-channel-models-for-60-ghz-wlan-systems.doc

[11] M. P. Fossorier, F. Burkert, S. Lin, and J. Hagenauer, "On the equivalence between SOVA and max-log-MAP decodings," *Communications Letters, IEEE*, vol. 2, no. 5, pp. 137–139, 1998.

[12] Balatsoukas-Stimming *et al.*, "A parallelized layered QC-LDPC decoder for IEEE 802.11 ad," in *New Circuits and Systems Conference (NEWCAS), 2013 IEEE 11th International*. Ieee, 2013, pp. 1–4.